


Article

Mechanical Activation-Assisted Solid-State Aluminothermic Reduction of CuO Powders for In-Situ Copper Matrix Composite Fabrication

Sahand Arasteh¹, Afshin Masoudi^{1,*}, Alireza Abbasi¹ and Saeid Lotfian^{2,*} 

¹ Department of Materials Engineering, Science and Research Branch, Islamic Azad University, Tehran 1477893855, Iran; araste.sahand@yahoo.com (S.A.); alireza.abbasi@srbiau.ac.ir (A.A.)

² Faculty of Engineering, University of Strathclyde, Glasgow G1 1XQ, UK

* Correspondence: a.masoudi@srbiau.ac.ir (A.M.); saeid.lotfian@strath.ac.uk (S.L.);
Tel.: +44-(0)-141-5484371 (S.L.)

Abstract: In this study, combustion synthesis involving mechanical milling and subsequent sintering process was utilised to fabricate Cu/Al_xCu_y/Al₂O₃ in-situ composite through the aluminothermic reduction of CuO powders. First, CuO and Al powders were mixed, and ball milled for 30–150 min to facilitate self-propagating high-temperature synthesis (SHS). Then, mechanically activated Al-CuO powders were mixed with elemental Cu powders and experienced subsequent cold compaction and sintering processes. The reactions during synthesis were studied utilising differential thermal analysis (DTA), X-ray diffraction (XRD), and scanning electron microscopy (SEM). Densification and hardness of green and sintered bodies were also obtained. The results indicated that despite the negative free energy of the aluminothermic reaction, an initial activation energy supply is required, and mixed Al-CuO powders did not show significant progress in the combustion synthesis method. The aluminothermic reaction became probable whenever the activation energy was entirely provided by high-energy ball milling or by the sintering of ball-milled Al-CuO mixed powders. DTA results showed that the aluminothermic reaction temperature of Al-CuO decreased with milling times, whereas after 150 min of ball milling, the reaction was completed. XRD patterns revealed that the formation of Al₂Cu and Al₂O₃ reinforcing phases resulted from CuO reduction with Al. Al₄Cu₉, Cu solid solution, and Al oxide phases were observed in sintered samples. The relative density of the samples was reduced compared to the green compacted parts due to the nature of the Cu-Al alloy and the occurrence of the swelling phenomenon. The hardness results indicated that in-situ formation of reinforcing phases in samples that experienced thermally assisted thermite reaction yielded superior hardness.

Keywords: in-situ composite; aluminothermic reduction; powder metallurgy; combustion synthesis; mechanical activation



Citation: Arasteh, S.; Masoudi, A.; Abbasi, A.; Lotfian, S. Mechanical Activation-Assisted Solid-State Aluminothermic Reduction of CuO Powders for In-Situ Copper Matrix Composite Fabrication. *Metals* **2022**, *12*, 1292. <https://doi.org/10.3390/met12081292>

Academic Editors: Roberto Figueiredo and Eric Mazzer

Received: 30 May 2022

Accepted: 28 July 2022

Published: 31 July 2022

Publisher's Note: MDPI stays neutral with regard to jurisdictional claims in published maps and institutional affiliations.



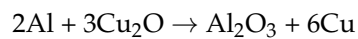
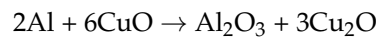
Copyright: © 2022 by the authors. Licensee MDPI, Basel, Switzerland. This article is an open access article distributed under the terms and conditions of the Creative Commons Attribution (CC BY) license (<https://creativecommons.org/licenses/by/4.0/>).

1. Introduction

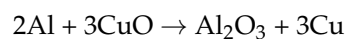
The fabrication of metal matrix composites (MMC) through conventional methods can frequently lead to several considerable challenges, including the wettability of reinforcing particles and the uncontrollable reaction between particle and matrix that results in an inappropriate distribution of particles [1]. However, the in-situ approach is one new technique for producing metal-matrix composites in which the reinforcing phase is formed through a chemical reaction between precursor materials in the matrix [2–7]. Therefore, the reinforcement is uniformly dispersed, and greater compatibility can be seen in the matrix [8–10]. Among the in-situ preparation methods, self-propagating high-temperature synthesis (SHS) is a promising process capable of fabricating composite materials through exothermic reactions such as aluminothermic reduction [11–14]. The SHS method, sometimes known as internal oxidation, has been extensively employed to fabricate reinforcements, which are

difficult to manufacture by conventional methods due to their high formation temperature in the metal matrix composites [15]. Therefore, ceramic reinforcements, such as oxides or intermetallics, are suitable candidates for SHS processing. SHS has the advantages of a high production rate, low energy consumption, simple process, and low cost [16].

Recently, several efforts have been made to fabricate in-situ composites with Al₂O₃ reinforcement through the aluminothermic reduction of various metal oxides. Chen et al. [17] reported a chemical reaction between ZnO and molten aluminium, which led to the formation of very fine Al₂O₃ particles and the dissolved elemental zinc in the aluminium matrix composite. Roy et al. [18] prepared Al matrix composites reinforced with well-dispersed Al₂O₃ and Ti-aluminide crystallites by hot pressing of Al and nano TiO₂ particles. One another vastly used oxide in aluminothermy is CuO [19]. In the Al-CuO system, the reduced Cu can be dissolved to some extent in the Al matrix and, at the same time, react with the Al to form an intermetallic phase that can reinforce the matrix of the composite [20]. Alam et al. [21] evaluated the Al-CuO thermite reaction and proposed that the in-situ process can take place in two succeeding reactions consisting of [20–23]:



They concluded that these reactions could be combined into:



Aluminothermic reduction of CuO particles has been used successfully in molten aluminium [24]. Zhao et al. [25] used a displacement reaction between Al and CuO powders at 900 °C to produce an in-situ Al₂O₃ reinforced Al(Cu) matrix composite. By utilising a weight ratio of 4:1 for Al to CuO powders, they reported Al₂Cu–Al(Cu) eutectic phase and Al₂O₃ particles along with the Al₂Cu phase. Shengqi et al. [26] investigated the solid-state mechanically activated aluminothermic reaction of CuO and observed a probable reduction of CuO during ball milling. The revealed final composite products were Cu + Al₂O₃, Cu₉Al₄ + Al₂O₃, CuAl₂ + Al₂O₃ and Al₂O₃ + Al(Cu) solid solution with increasing amounts of aluminium. A similar method was employed by Arami et al. [27]. They explored the effect of using high-energy attrition milling under a high purity argon atmosphere on the reaction between CuO and Al powders. They reported that the reaction was completed after 60 h and occurred immediately at a temperature of over 840 °C. Venugopal et al. [28] examined Cu/Al₂O₃ nanocomposite synthesis through reactive milling of Al-CuO powders for up to 20 h. They disclosed that the reduction extent increases with Al content. They inhibited the SHS reaction by means of using toluene as a milling medium, which resulted in the formation of nanostructured Cu and Al₂O₃.

Copper matrix composites have a wide range of applications comprising high electrical and thermal conductivities. Cu-Al₂O₃ composites are mostly used in electrode materials, especially spot welding [24,29–33]. These composites are ordinarily prepared by conventional powder metallurgy [34] or casting [35] routes. However, the in-situ reinforced Al₂O₃ can increase the strength and improve composites' tribological, electrical and thermal properties [36–39].

In the current study, attempts have been made to produce in-situ Al₂O₃ (and Al_xCu_y intermetallic) reinforced Cu matrix composite via a solid-state self-propagating high-temperature synthesis (SHS) method. Our main purpose in the current study is to lower the fabrication temperature of a copper matrix composite encompassing in-situ reinforcement phase(s) by conducting a preliminary mechanical activation. We believe hybrid in-situ reinforcements (compared with ex-situ reinforcing materials) may bring superior mechanical and physical properties. Here, we preferred to work with a reasonably high Al:CuO molar ratio (relatively similar mass contents) to mix powders better, leading to a more significant combustion synthesis reaction. On the other hand, to reduce the ignition temperature towards lower thermite temperatures in solid-state, mixed Al-CuO powders experienced an initial mechanical activa-

tion (high energy ball milling). The paper also describes the effect of synthesis temperature on phase transformations and subsequent obtained mechanical properties.

2. Materials and Methods

The as-received pure Aluminum powder (>99.0%, the average particle size of 20 μm , from Merck, Darmstadt, Germany) and CuO powder (99.9%, average particle size of 10 μm , Sigma Aldrich, Burlington, MA, USA) were mixed in an 8:3 molar ratio (0.91:1 weight ratio) for 1 h in a Turbula mixer at the first preparation step. The mixed powders were subsequently milled for 30, 90 and 150 min using a planetary high energy ball mill (MPM 2 \times 250 H) operating at 300 RPM with a 10:1 ball to powder ratio. Milling was performed under Ar protective gas, in a dry medium, and with hardened stainless steel vials and hardened steel balls. Once again, using a Turbula Mixer, ball-milled powders were mixed with Cu powders (99.8%, average particle size of 20 μm , Merck, Darmstadt, Germany) as composite matrix material in a 2:1 molar ratio with starting Al powder. Then, the blended powders were cold pressed under 450 MPa uniaxial load to form cylinders with 20 mm height and 20 mm diameter.

Finally, green compacts were sintered in a pressureless manner at different furnace temperatures of 650, 750 and 850 $^{\circ}\text{C}$ under Ar gas atmosphere for 2 h. A schematic illustration of the entire process is depicted in Figure 1. The name of the designed samples is tabulated in Table 1.

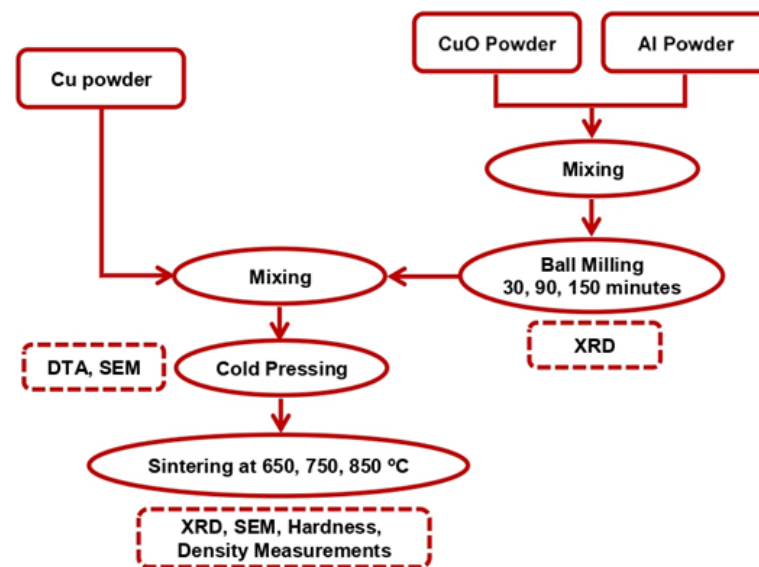


Figure 1. Schematic flow diagram of the synthesis process.

Table 1. Synthesis conditions and related code for milled powders and sintered samples.

| No. | Milling Time (Min) | Sintering Temperature ($^{\circ}\text{C}$) | Sample Code | |
|-----|--------------------|--|----------------|-----------------|
| | | | Milled Powders | After Sintering |
| 1 | 30 | 650 | C1 | C1T1 |
| 2 | | 750 | | C1T2 |
| 3 | | 850 | | C1T3 |
| 4 | 90 | 650 | C2 | C2T1 |
| 5 | | 750 | | C2T2 |
| 6 | | 850 | | C2T3 |
| 7 | 150 | 650 | C3 | C3T1 |
| 8 | | 750 | | C3T2 |
| 9 | | 850 | | C3T3 |

The flow diagram also shows characterisation methods that have been executed in different preparation stages of the composite. Possible phase evolutions after ball milling of Al/CuO powders and for sintered samples were studied by X-ray diffraction (XRD, Panalytical 40 kV, 40 mA, Cu $K\alpha$ radiation, Malvern, Worcestershire, UK). Differential thermal analysis (DTA, SDT Q600 V20.9 Build 20, Milford, MA, USA) with a 10 °C/min heating rate was implemented as one suitable tool to evaluate the ignition temperature where thermite reaction between Al and CuO powders in the matrix of Cu powder can occur. Optical (BX51M-Olympus, Olympus Corporation, Tokyo, Japan) and scanning electron microscopes (SEM, FEI ESEM QUANTA 200, Hillsboro, OR, USA) were also used to explore the morphological and microstructural changes during the synthesis procedure. No etchant solution was used for SEM imaging. Energy dispersive spectrometry (EDS, EDAX Silicon Drift 2017, Ametek, Berwyn, PA, USA) assisted microstructural investigations. Density measurement was performed according to Archimedes' principle. For precise weight measurements, the surface of the samples was covered with wax. Vickers hardness test (Zwick Roell, Ulm, Germany) at the load of 20 kgf. was also carried out to evaluate changes in mechanical properties during different stages of the process.

3. Results and Discussion

It is well recognised that high-energy ball milling can considerably affect powder reactivity by so-called mechanical activation [25]. Chemical, structural and morphological transformations are expected to occur because of intimate contact of starting powder and the repetitive cold-weld process. Figure 2a–c represents an SEM micrograph of precursor materials. Al and CuO particles were relatively spherical. However, electrodeposited Cu powder showed dendritic morphology.

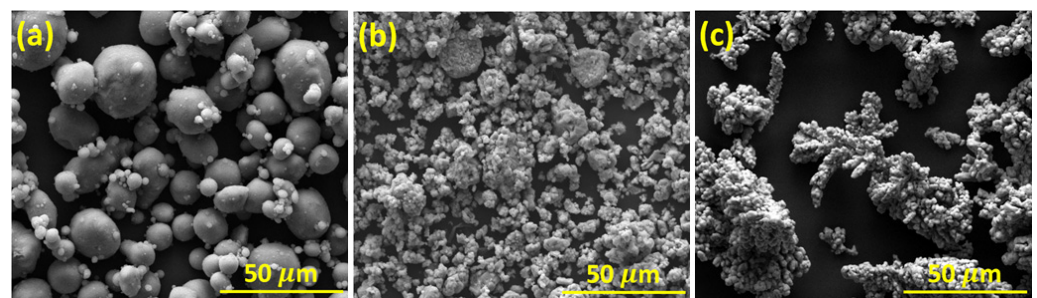


Figure 2. SEM micrograph of starting powders (a) Al, (b) CuO, and (c) Cu.

The spherical shape of Al and CuO powders gradually changed to a flattened appearance after 30 min and demonstrated elongated and wrinkled structure in longer milling times (Figure 3a,b). It should be noted that in the early stages of mechanical activation, Al particles can deform and resize due to the effect of impacting balls. At the same time, the brittle CuO powder particles plunge into the Al soft phase. As the milling process continues, Al particles become harder because of work hardening and CuO reinforcing mechanisms, and the size of Al particles decreases. EDS analysis showed that the crushed CuO particles have been interred to the surface of the Al particles and covered the particles' surfaces. Therefore, high energy ball milling resulted in the formation of a composite powder in such a way that after 90 min, identifying the Al and CuO powders was quite difficult.

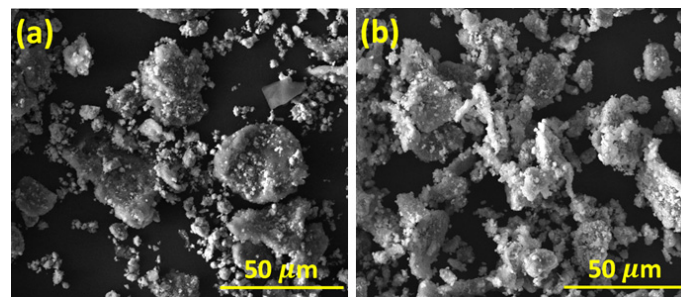


Figure 3. SEM micrograph of Al-CuO powders after (a) 30 and (b) 90 min of ball milling.

Figure 4 displays XRD patterns of raw materials and resulting powders obtained from different ball milling times. XRD patterns of pure aluminium and copper oxide (CuO) powders have been prepared for better comparison. One can conclude that the intensity of related aluminium peaks was gradually decreased with milling, which could be a consequence of powder fragmentation. A similar intensity reduction was observed in CuO particles.

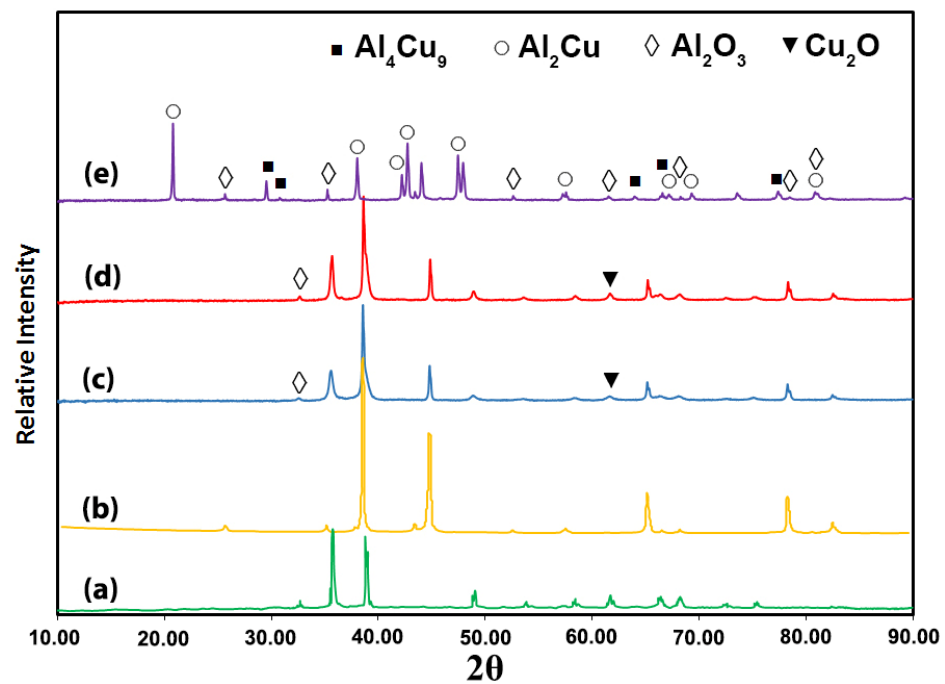
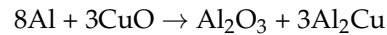


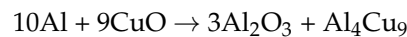
Figure 4. XRD patterns of starting materials (a) copper oxide, (b) aluminium, and mixed powders after different milling times of (c) 30 (C1), (d) 90 (C2), and (e) 150 (C3) min.

As shown in Figure 4c, the characteristic peaks of Al_2O_3 , CuO, Cu_2O , and Al can be identified in the C1 sample that experienced 30 min of high-energy ball milling. However, the intensity of Al peaks was reduced in a higher milling time of 90 min (Figure 4d) and completely disappeared after 150 min (Figure 4e). The presence of a characteristic peak of Cu_2O in lower milling times may be attributed to the partial reduction of CuO particles during the ball milling. The produced Cu_2O phase, further reduced by Al particles at much longer times, has been observed. XRD results indicated that in the C3 sample with 150 min of ball-milled (Figure 4e), CuO peaks were annihilated, which may be related to the complete reduction of CuO by Al particles during the milling and occurring a mechanically induced combustion synthesis reaction in solid state. As a result of CuO reduction, intermetallic compounds such as Al_2Cu were likely to form. Moreover, the corresponding representative peaks of Al_2O_3 were more noticeable (Figure 4e) after 150 min of milling.

These results are in good agreement with previous findings of other researchers that proposed a two-step reduction of CuO by Al particles via an intermediate phase and final Al₂O₃ product [10–13]. However, regarding the molar ratio of precursor materials in this study and analysis of produced phases, suggested possible reactions during the milling process can be:



Another in-situ formed phase from the aluminothermic reaction in the extended milling time was Al₄Cu₉, a thermodynamically stable phase, unlike the metastable AlCu phase (it was not detected). Al₄Cu₉ phase can be produced in regions with locally lower available aluminium content through a possible reaction of:



It should be noted that Al₄Cu₉ formation may accompany a higher magnitude of alumina compared to the reaction of the formation of Al₂Cu. We believe that no evidence of intermetallic phases was discovered in moderate milling times (C1 and C2 samples), which indicates the incomplete or partial reduction of CuO. Al peaks were also observed in these conditions besides the copper oxides.

Figure 5 and the corresponding EDS chemical analysis in Table 2 demonstrate the microstructure of cold compacted samples comprising blended Cu particles with ball-milled Al-CuO powders. Different microstructure phase identification was performed by adapting the atomic ratios obtained from EDS analysis to X-ray results of milled powders (Figure 4). The presence of remaining Cu₂O and Al particles from starting materials adjacent to Cu particles was perceived in the C1 sample. Furthermore, copper oxides were also detected along with unreacted Al particles in the C2 sample. The resulting microstructures were different for the C3 sample, and the formation of an unstable Al₃Cu₂ phase was discovered. Al₃Cu₂ was mainly observed within Al₂Cu intermetallic phase due to the aluminothermy reaction. The formation of such hard and brittle intermetallic compounds is influenced by thermodynamics and kinetics of the aluminothermic reaction and mechanical or chemical activation. As mentioned earlier, many different chemical reactions can take place between aluminium, copper oxide and their newly formed intermetallic compounds. The competition between these reactions, in terms of reaction rate and type of prevailing mechanism, determines the predominant intermetallic composition. Despite the detrimental effect of these intermetallics on the ductility of reinforced composites, their formation is inevitable in the selected production conditions. Al₂O₃ particles were seen as a dark grey colour phase in Figure 5c. According to SEM microstructures and XRD patterns, it can be expressed that a complete aluminothermic reaction has happened during 150 min of powder milling.

The effect of high-energy ball milling on combustion synthesis via aluminothermic reaction was studied by differential thermal analysis (DTA) of cold-pressed samples, including Cu particles blended with ball-milled Al-CuO powders. For comparative assessment, unmilled mixed Cu-Al-CuO powders were also cold-pressed, and the relating DTA diagram was plotted.

Figure 6 shows the corresponding DTA diagram for different samples. Various exothermic or endothermic peaks revealed by DTA can better understand reaction temperature and the associated heat of reaction (enthalpy) regarding the amount of tested material. Removal of moisture and crystalline water from aluminium and copper oxide compounds has occurred up to temperatures of about 238 °C and can be seen in all diagrams as endothermic peaks. As shown in Figure 6a, endothermic peaks of Al melting and subsequent dissolution of copper in molten Al were evident at 667 and 822 °C, respectively. However, no evidence of exothermic thermite reaction can be recognised in unmilled powders. Considering the thermodynamic anticipations and temperatures well above the melting point of Al, it could be concluded that the only mixing process is insufficient for combustion synthesis. Figure 6b denotes an exothermic, very weak peak determining the possible

aluminothermic reaction at 934 °C for the C1 sample with 30 min of Al-CuO ball milling, again at temperatures higher than the melting point of Al.

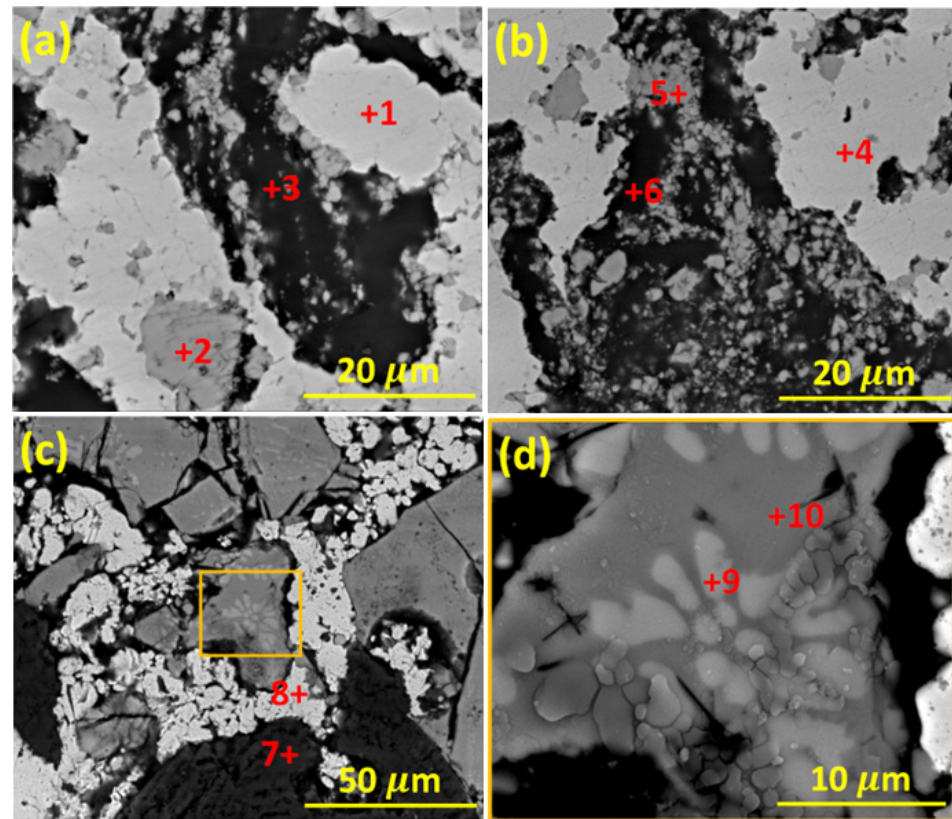


Figure 5. Backscattered SEM micrograph of cold-pressed samples comprising differently milled powders (a) C1, (b) C2, (c) C3, and (d) higher magnification of C3 smaller intersect.

Table 2. EDS analysis corresponding to related points of Figure 5.

| Figure 5 | Point | Atomic Percent (%) | | | Phase |
|----------|-------|--------------------|-------|-------|---------------------------------|
| | | Cu | Al | O | |
| a | 1 | 95.77 | 4.23 | - | Cu(α) |
| a | 2 | 65.06 | 2.93 | 32.01 | Cu ₂ O |
| a | 3 | 3.15 | 96.24 | 0.62 | Al |
| b | 4 | 91.93 | 8.07 | - | Cu(α) |
| b | 5 | 38.4 | 4.54 | 57.06 | CuO |
| b | 6 | 0.91 | 94.55 | 4.54 | Al |
| c | 7 | 0.93 | 56.97 | 42.1 | Al ₂ O ₃ |
| c | 8 | 94.46 | 3.24 | 2.3 | Cu(α) |
| d | 9 | 42.23 | 57.77 | - | Al ₃ Cu ₂ |
| d | 10 | 33.91 | 66.09 | - | Al ₂ Cu |

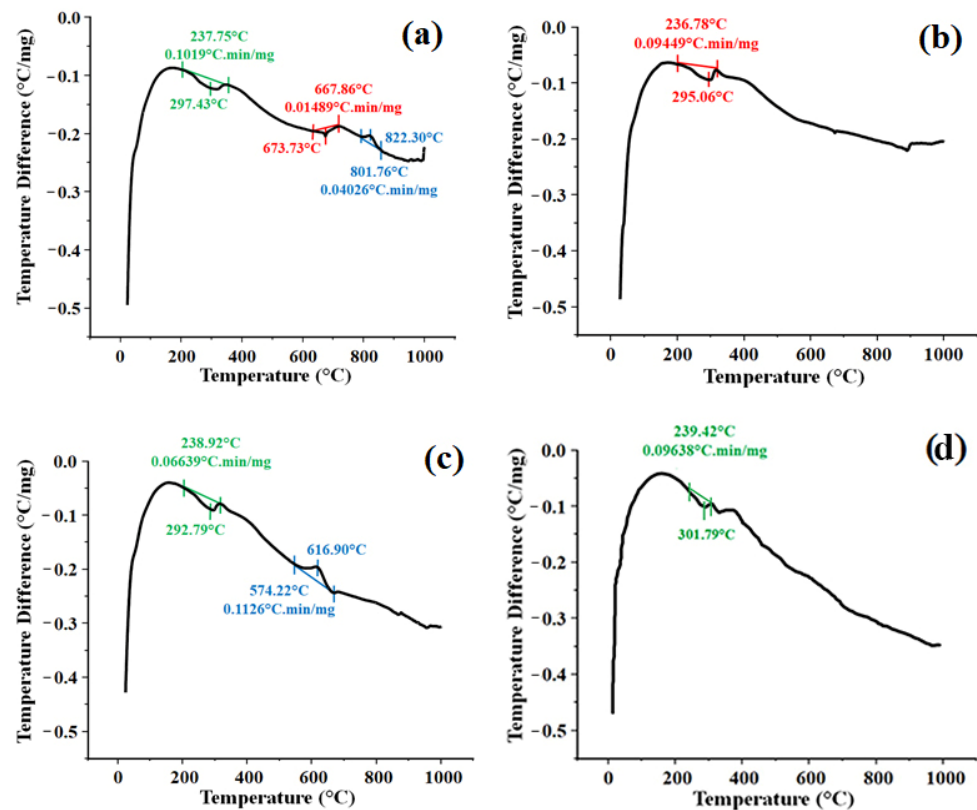


Figure 6. Differential thermal analysis (DTA) of cold-pressed (a) unmilled mixed, (b) C1, (c) C2 and (d) C3 samples.

Nonetheless, a completely different behaviour was exhibited by the C2 sample. The DTA results disclosed an exothermic peak at 616 °C, below the melting point of Al. Therefore, we can deduce that mechanical activation utilising high-energy ball milling will give rise to lower ignition temperature for thermite combustion synthesis. More inadequate thermite reactions may be attributed to superior energy conducted by high-energy milling. As previously discerned in the C3 sample, much higher mechanical energy at longer times caused a complete aluminothermic reaction without external thermally assisted processes. No appreciable effect for the occurrence of aluminothermic reactions can be seen in Figure 6d for the C3 sample.

Additionally, enthalpy is a valuable parameter that can be calculated by multiplying the area under the DTA curve by an experimental constant. The area yielded by the differential temperature curve integration is proportional to the heat absorbed or evolved by the sample. Therefore, the heat involved (ΔH) can be expressed by the equation [40,41]:

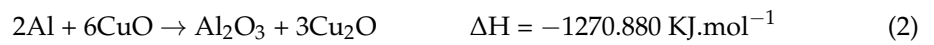
$$\Delta H = \varnothing \int_{t_1}^{t_2} \Delta T dt \quad (1)$$

where \varnothing is the proportionality constant that relates to the area of the DTA curve, t_1 , t_2 are temperature limits of the integral, and ΔT is a qualitative term concerning ΔH , a quantitative result.

Accordingly, by calculating the area under the curve of Figure 6c at 616 °C and considering the mass of the material (5.090 mg), we have:

$$\Delta H = -0.266 \text{ J.g}^{-1} = -7.19 \text{ J.mol}^{-1} \text{ Al}$$

For the solid-state thermite reaction, the enthalpy of predominant thermite reactions in the two-step mechanism, including reactions (2) and (3) at 616 °C, are:



Therefore, regarding the amount of 1.07 mg of primary aluminium in the powder mixture used in the DTA test and using the law of proportions, one can conclude that 29.91% of preliminary Al has participated in the thermite reaction. The EDS analysis and XRD pattern can explain this before sintering for sample C2.

Figure 7 shows the effect of sintering temperature on the microstructure of compacted samples fabricated from a mixture of Cu and milled powders. A sample was also prepared from unmilled powders for comparison. Figure 7 illustrates the SEM micrographs, and corresponding EDS analysis results have been tabulated in Table 3. Sintering of the compacted sample from unmilled powders at 750 °C yielded Cu(α) matrix with intermediate oxide compounds between Cu and Al. It revealed that in non-activated samples, the aluminothermic reduction of CuO in the matrix of Cu particles was rather difficult, even in the molten phase and 2 h of sintering. The result was a copper matrix with Cu-Al dual oxide particles.

In the case of the C1T2 sample obtained from the powders, which did not show considerable progress in thermite reaction due to shorter milling time, Al₄Cu₉ intermetallic phase and Cu-Al dual oxide were observed. A very fine structure of eutectoid transformation was also discovered, but the distribution of resultant phases was quite inhomogeneous. Such a structure may be related to an incomplete thermite reaction after the sintering process.

The eutectoid structure consisting of Cu and Al₄Cu₉ phases has been better identified in C2 samples sintered at different temperatures. This microstructure was vastly distributed all over the sample and may be attributed to thermally assisted thermite reaction via the sintering process. The eutectoid structure may originate from Al₄Cu₉ and Cu(α) formation from other intermetallic phases.

After sintering, the C3 sample that endured the complete thermite reaction during ball milling represented a similar eutectoid structure. The main difference for this sample is that the amount of eutectoid structure is less than that of the C2 specimens.

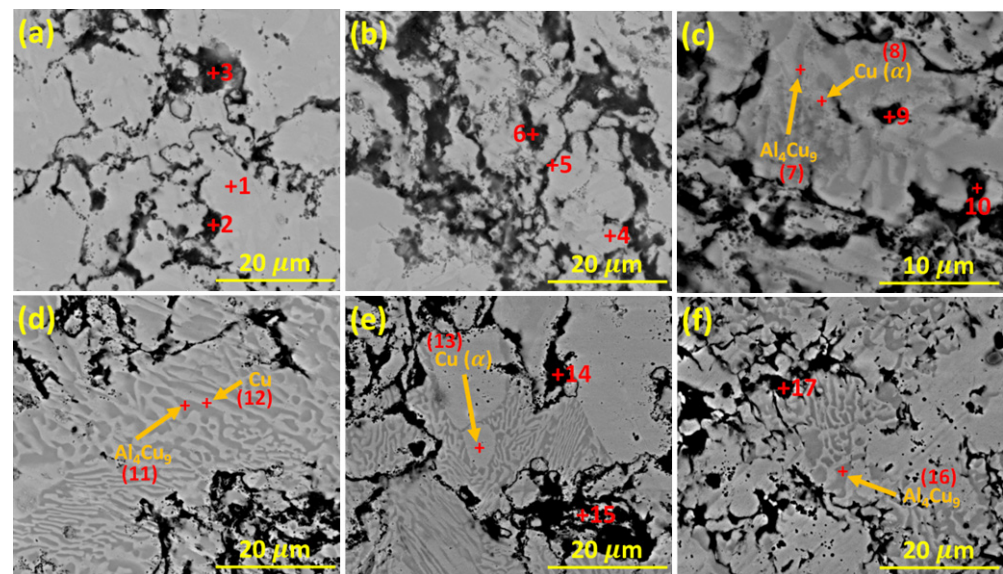
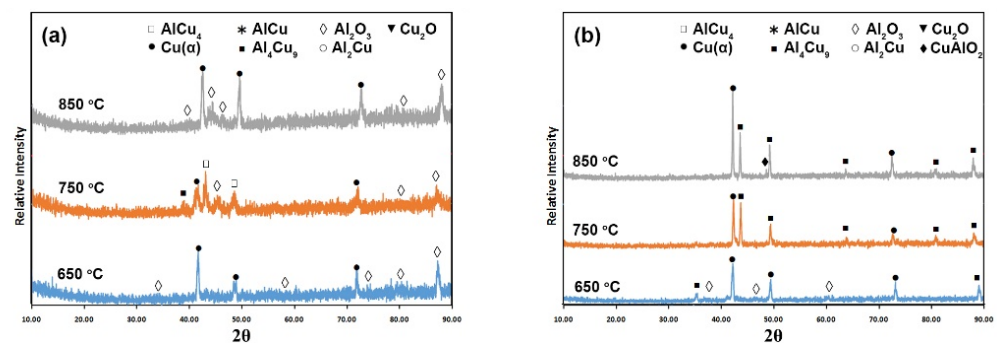


Figure 7. Backscattered SEM micrograph of compacted samples after sintering, (a) unmilled powder at 750 °C, (b) C1T2, (c) C2T1, (d) C2T2, (e) C2T3, and (f) C3T2.

Table 3. EDS analysis of corresponding samples of Figure 7.

| Figure 7 | Point | Atomic Percent (%) | | | Phase |
|----------|-------|--------------------|-------|-------|--|
| | | Cu | Al | O | |
| a | 1 | 70.48 | 29.52 | - | Cu(α) |
| a | 2 | 16.36 | 41.67 | 41.98 | CuAl ₂ O ₂ |
| a | 3 | 7.66 | 42.54 | 49.8 | CuAl ₄ O ₅ |
| b | 4 | 69.52 | 30.48 | - | Al ₄ Cu ₉ |
| b | 5 | 17.8 | 33.69 | 48.51 | Cu ₂ Al ₃ O ₅ |
| b | 6 | 23.88 | 37.35 | 38.77 | CuAl ₂ O ₂ |
| c | 7 | 69.68 | 30.32 | - | Al ₄ Cu ₉ |
| c | 8 | 77.44 | 22.56 | - | Cu(α) |
| c | 9 | 42.53 | 23.53 | 33.94 | Cu ₄ Al ₂ O ₃ |
| c | 10 | 35.58 | 26.82 | 37.61 | Cu ₇ Al ₅ O ₇ |
| d | 11 | 65.7 | 34.3 | - | Al ₄ Cu ₉ |
| d | 12 | 73.09 | 26.91 | - | Cu(α) |
| e | 13 | 76.14 | 23.86 | - | Cu(α) |
| e | 14 | 35.58 | 29.83 | 34.59 | Cu ₇ Al ₆ O ₇ |
| e | 15 | 39.27 | 33.41 | 27.32 | Cu ₄ Al ₃ O ₃ |
| f | 16 | 65.41 | 34.59 | - | Al ₄ Cu ₉ |
| f | 17 | 45.71 | 28.89 | 25.4 | CuAl ₂ O ₂ |

XRD patterns of C2 and C3 samples sintered at different temperatures are illustrated in Figure 8. XRD results showed that C2 sintered samples mainly comprised Cu(α) and Al₂O₃ phases. Detection of Al₂O₃ peaks in C2 samples may imply that thermite reduction has been continued after sintering. However, for the C3 sample that experienced a complete aluminothermic reaction during mechanical activation, the formerly produced Al₂O₃ phase was present in the sintering process. Except for C3T1, two other samples which endured higher sintering temperatures did not show free Al₂O₃. It may be attributed to the incorporation of Al₂O₃ into different copper-bearing phases. Characteristic diffraction peaks of Al₄Cu₉ revealed that it was the dominant reinforcing phase in the C3 sample. CuAlO₂ was also perceived for C3T3 sintered samples. The XRD results were in good agreement with the EDS analysis.

**Figure 8.** XRD pattern of sintered samples (a) C2 and (b) C3 at different temperatures.

The green density of cold-pressed samples and sintered ones are gathered in Figure 9. Unmilled powders demonstrated considerably higher green density because of the spherical shape of enclosing powders. Green density decreased with milling up to 90 min. On the other hand, Figure 9 indicated a decrease followed by an increase in the density of the sintered samples. Samples sintered from powders that had undergone the initial stages of milling (30 and 90 min) demonstrated a decrease in density. However, in the samples obtained from powders with longer milling time (C3, 150 min), an increasing trend is seen in density. It has been concluded that the lower sintered density of copper powder compacts compared to green densities can be linked to the swelling mechanism observed by other researchers [42]. This may be attributed to the infiltration of the molten material

into the solid grains. The Al-Cu equilibrium diagram can explain the phenomena. This may be attributed to the infiltration of the molten material into the solid grains. The Al-Cu equilibrium diagram can explain the phenomena. Swelling is a common aspect of sintering in copper and its alloys [43], which can be suppressed by heating the samples under pressure to minimise or prevent voids formation and swelling [44] (which has not been applied in this study). Successful sintering with considerable condensation requires dissolving one component (usually matrix) in other constituents. However, in this study, with the Cu matrix, since the ratio of the volume fraction of Cu dissolution in Al to Al dissolution in Cu (According to the equilibrium diagram) was smaller than one, the phenomenon of swelling can be observed in the samples. By increasing the sintering temperature, the effect of swelling and the difference in the green density became more apparent, which shows the impact of higher temperature on the swelling phenomenon. However, the samples obtained from powder milled for longer times showed a less swelling effect. Angular and flattened particles provided more space for melt infiltration and displayed lower swelling. Higher mechanical milling that can induce high melting point reinforcement phases (such as intermetallics and oxide phases) may hinder the swelling.

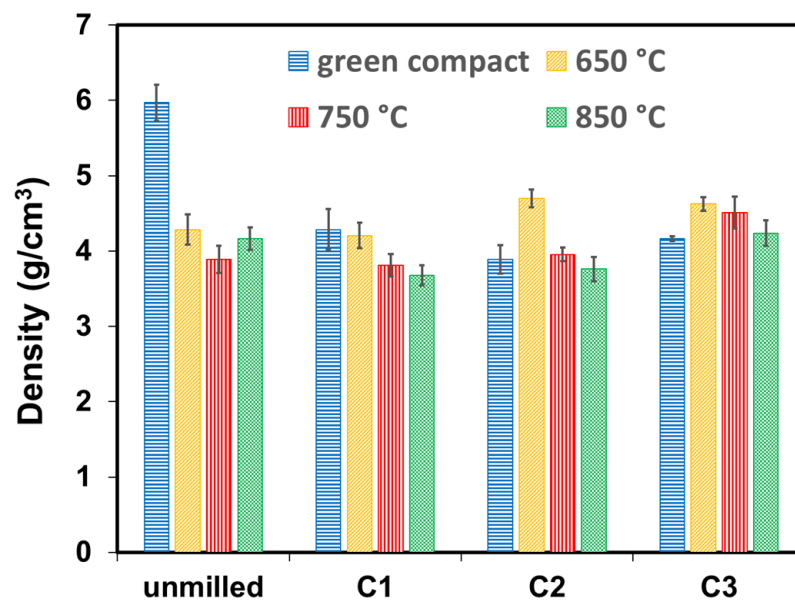


Figure 9. The density of green and sintered samples were prepared from powders with different milling times.

The Vickers hardness results are depicted in Figure 10. Hardness was superior for C2 samples, those with thermally induced aluminothermic reaction. C1 samples also demonstrated higher hardness values compared to C3 samples, which showed a complete thermite reaction during milling. It can be concluded that the in-situ formation of Al_2O_3 and significant eutectoid transformation comprising intermetallic Al_4Cu_9 phases in the sintering process may lead to more rigid structures. On the other hand, the lowest hardness level was related to the unmilled sample. Lower densities for samples with longer milling time caused inferior hardness.

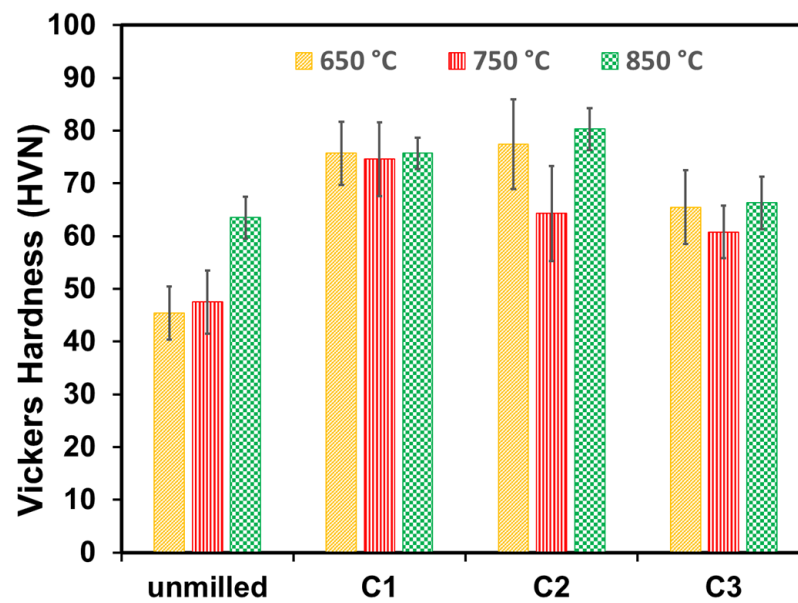


Figure 10. The hardness of sintered samples.

4. Conclusions

An in-situ Cu matrix composite was prepared through an aluminothermic reduction of CuO powders. The starting powders were ball milled to prepare an intimate contact between Al and CuO. Milled powders were blended with Cu, followed by cold compaction and sintering processes.

- The results indicated that 150 min of ball milling could lead to a complete thermite reaction with resultant products of Al_2O_3 and Al_2Cu phases. However, aluminothermy was not mechanically activated in shorter times.
- DTA results showed that, using high-energy ball milling, subsequent ignition temperature during the sintering process decreased to lower temperatures.
- A eutectoid phase comprising Al_4Cu_9 and Cu solid solution and the Al oxide phase was observed in sintered samples.
- Density measurement evaluations showed a swelling phenomenon that was more significant at higher sintering temperatures. Swelling decreased in samples prepared from flattened and angular ball-milled powders.
- In-situ reinforcing phases in samples that experienced thermally assisted thermite reaction led to superior hardness.

Author Contributions: Conceptualization, S.A., A.M., A.A. and S.L.; methodology, A.M. and A.A.; validation, S.A., A.M. and A.A.; formal analysis, S.A., A.M., A.A. and S.L.; investigation, S.A., A.M., A.A. and S.L.; resources, A.M., A.A. and S.L.; data curation, S.A., A.M. and A.A.; writing—original draft preparation, S.A.; writing—review and editing, S.A., A.M., A.A. and S.L.; visualization, S.A., A.M. and A.A.; supervision, A.M., A.A. and S.L.; project administration, A.M.; funding acquisition, S.L. All authors have read and agreed to the published version of the manuscript.

Funding: This work was supported by the Centre for Advanced Materials for Renewable Energy Generation (CAMREG) under grant number EP/P007805/1 from the UK Engineering and Physical Sciences Research Council (EPSRC).

Data Availability Statement: The data presented in this study are available on request from the corresponding author. The data are not publicly available because it also forms part of an ongoing study.

Conflicts of Interest: The authors declare no conflict of interest.

References

1. Chawla, K.K. *Composite Materials: Science and Engineering*; Springer Science & Business Media: Berlin, Germany, 2012.
2. Huang, Z.; Yang, B.; Cui, H.; Duan, X.; Zhang, J. Microstructure of designed Al matrix composites reinforced by combining in situ alloying elements and Al₂O₃ (p). *J. Mater. Sci. Lett.* **2001**, *20*, 1749–1751. [[CrossRef](#)]
3. Chaudhury, S.; Singh, A.; Sivaramkrishnan, C.; Panigrahi, S. Preparation and thermomechanical properties of stir cast Al-2Mg-11TiO₂ (rutile) composite. *Bull. Mater. Sci.* **2004**, *27*, 517–521. [[CrossRef](#)]
4. Azimi-Roeen, G.; Kashani-Bozorg, S.F.; Nosko, M.; Švec, P. Reactive mechanism and mechanical properties of in-situ hybrid nano-composites fabricated from an Al-Fe₂O₃ system by friction stir processing. *Mater. Charact.* **2017**, *127*, 279–287. [[CrossRef](#)]
5. AzimiRoeen, G.; Kashani-Bozorg, S.F.; Nosko, M.; Lotfian, S. Mechanical and microstructural characterisation of hybrid aluminum nanocomposites synthesised from an Al-Fe₃O₄ system by friction stir processing. *Met. Mater. Int.* **2020**, *26*, 1441–1453. [[CrossRef](#)]
6. Guo, S.; Zhang, X.; Shi, C.; Zhao, D.; Liu, E.; He, C.; Zhao, N. Comprehensive performance regulation of Cu matrix composites with graphene nanoplatelets in situ encapsulated Al₂O₃ nanoparticles as reinforcement. *Carbon* **2022**, *188*, 81–94. [[CrossRef](#)]
7. Rashidi, K.; Moazami-Goudarzi, M.; Masoudi, A. Powder processing, characterisation and mechanical properties of Al/GNP composites. *Mater. Chem. Phys.* **2020**, *256*, 123719. [[CrossRef](#)]
8. Reddy, B.; Das, K.; Das, S. A review on the synthesis of in situ aluminum based composites by thermal, mechanical and mechanical–thermal activation of chemical reactions. *J. Mater. Sci.* **2007**, *42*, 9366–9378. [[CrossRef](#)]
9. Chen, Z.-C.; Takeda, T.; Ikeda, K. Microstructural evolution of reactive-sintered aluminum matrix composites. *Compos. Sci. Technol.* **2008**, *68*, 2245–2253. [[CrossRef](#)]
10. Odhiambo, J.O.; Yoshida, M.; Otsu, A.; Yi, L.-F.; Onda, T.; Chen, Z.-C. Microstructure and tensile properties of in-situ synthesised and hot-extruded aluminum-matrix composites reinforced with hybrid submicron-sized ceramic particles. *J. Compos. Mater.* **2022**, *56*, 1987–2001. [[CrossRef](#)]
11. Corbin, N.; McCauley, J. *Self-Propagating High-Temperature Synthesis (SHS): Current Status and Future Prospects. Final Report*; US Department of Energy Office of Scientific and Technical Information: Oak Ridge, TN, USA, 1986.
12. Rong, X.; Zhao, D.; He, C.; Shi, C.; Liu, E.; Zhao, N. Revealing the strengthening and toughening mechanisms of Al-CuO composite fabricated via in-situ solid-state reaction. *Acta Mater.* **2021**, *204*, 116524. [[CrossRef](#)]
13. Rosa, R.; Veronesi, P.; Leonelli, C. 4—Use of combustion synthesis/self-propagating high-temperature synthesis (SHS) for the joining of similar/dissimilar materials. In *Joining Processes for Dissimilar and Advanced Materials*; Rakesh, P., Davim, J.P., Eds.; Woodhead Publishing: Sawston, UK, 2022; pp. 63–79.
14. Matveev, A.; Promakhov, V.; Nikitin, P.; Babaev, A.; Vorozhtsov, A. Effect of Mechanical Activation of Al-Ti-B Powder Mixture on Phase Composition and Structure of Al-TiB₂ Composite Materials Obtained by Self-Propagating High-Temperature Synthesis (SHS). *Materials* **2022**, *15*, 2668. [[CrossRef](#)]
15. Mishra, S.K.; Pathak, L. Self-propagating high-temperature synthesis (SHS) of advanced high temperature materials. In *Proceedings of the Indo-Malaysian Joint Workshop (WAM-2002)*, Jamshedpur, India, 12–13 March 2002; p. 107.
16. Tjong, S.; Ma, Z. Microstructural and mechanical characteristics of in situ metal matrix composites. *Mater. Sci. Eng. R Rep.* **2000**, *29*, 49–113. [[CrossRef](#)]
17. Chen, G.; Sun, G.-X. Study on in situ reaction-processed Al-Zn/ α -Al₂O₃ (p) composites. *Mater. Sci. Eng. A* **1998**, *244*, 291–295. [[CrossRef](#)]
18. Roy, D.; Ghosh, S.; Basumallick, A.; Basu, B. Preparation of Ti-aluminide reinforced in situ aluminium matrix composites by reactive hot pressing. *J. Alloy. Compd.* **2007**, *436*, 107–111. [[CrossRef](#)]
19. Wang, D.; Shi, Z.; Hao, K.; Froyen, L. Aluminothermic reduction of Cu⁺⁺ in Al-CuO system. *J. Adv. Mater.* **2002**, *34*, 27–30.
20. Blobaum, K.; Wagner, A.; Plitzko, J.; Van Heerden, D.; Fairbrother, D.; Weihs, T. Investigating the reaction path and growth kinetics in CuO x/Al multilayer foils. *J. Appl. Phys.* **2003**, *94*, 2923–2929. [[CrossRef](#)]
21. Alam, S.N.; Sharma, N.; Panda, D.; Kumar, A.; Sampenga, D.; Sairam, A.; Sarky, V.; Krupateja, M. Mechanical milling of Al and synthesis of in-situ Al₂O₃ particles by mechanical alloying of Al-CuO system. *J. Alloy. Compd.* **2018**, *753*, 799–812. [[CrossRef](#)]
22. Takacs, L. Self-sustaining reactions induced by ball milling. *Prog. Mater. Sci.* **2002**, *47*, 355–414. [[CrossRef](#)]
23. Yang, B.; Sun, M.; Gan, G.; Xu, C.; Huang, Z.; Zhang, H.; Fang, Z.Z. In situ Al₂O₃ particle-reinforced Al and Cu matrix composites synthesised by displacement reactions. *J. Alloy. Compd.* **2010**, *494*, 261–265. [[CrossRef](#)]
24. Dash, K.; Panda, S.; Ray, B. Process and progress of sintering behavior of Cu-Al₂O₃ composites. *Emerg. Mater. Res.* **2013**, *2*, 32–38. [[CrossRef](#)]
25. Zhao, G.; Shi, Z.; Ta, N.; Ji, G.; Zhang, R. Effect of the heating rate on the microstructure of in situ Al₂O₃ particle-reinforced Al matrix composites prepared via displacement reactions in an Al/CuO system. *Mater. Des.* **2015**, *66*, 492–497. [[CrossRef](#)]
26. Shengqi, X.; Xiaoyan, Q.; Mingliang, M.; Jingen, Z.; Xiulin, Z.; Xiaotian, W. Solid-state reaction of Al/CuO couple by high-energy ball milling. *J. Alloy. Compd.* **1998**, *268*, 211–214. [[CrossRef](#)]
27. Arami, H.; Simchi, A.; Reihani, S.S. Mechanical induced reaction in Al-CuO system for in-situ fabrication of Al based nanocomposites. *J. Alloy. Compd.* **2008**, *465*, 151–156. [[CrossRef](#)]
28. Venugopal, T.; Rao, K.P.; Murty, B. Synthesis of copper-alumina nanocomposite by reactive milling. *Mater. Sci. Eng. A* **2005**, *393*, 382–386. [[CrossRef](#)]
29. Rajković, V.M.; Božić, D.; Popović, M.; Jovanović, M.T. The influence of powder particle size on properties of Cu-Al₂O₃ composites. *Sci. Sinter.* **2009**, *41*, 185–192. [[CrossRef](#)]

30. Korać, M.; Kamberović, Ž.; Anđić, Z.; Filipović, M.; Tasić, M. Sintered materials based on copper and alumina powders synthesised by a novel method. *Sci. Sinter.* **2010**, *42*, 81–90. [[CrossRef](#)]
31. Tash, M.M.; Mahmoud, E.R. Development of in-situ Al-Si/CuAl₂ metal matrix composites: Microstructure, hardness, and wear behavior. *Materials* **2016**, *9*, 442. [[CrossRef](#)]
32. Cao, H.; Zhan, Z.; Lv, X. Microstructure Evolution and Properties of an In-Situ Nano-Gd₂O₃/Cu Composite by Powder Metallurgy. *Materials* **2021**, *14*, 5021. [[CrossRef](#)]
33. Liu, K.; Sheng, X.; Li, Q.; Zhang, M.; Han, N.; He, G.; Zou, J.; Chen, W.; Atrons, A. Microstructure and Strengthening Model of Cu–Fe In-Situ Composites. *Materials* **2020**, *13*, 3464. [[CrossRef](#)] [[PubMed](#)]
34. Rajkovic, V.; Bozic, D.; Jovanovic, M.T. Effects of copper and Al₂O₃ particles on characteristics of Cu–Al₂O₃ composites. *Mater. Des.* **2010**, *31*, 1962–1970. [[CrossRef](#)]
35. Soleimanpour, A.; Abachi, P.; Purazrang, K. Wear behaviour of in situ Cu–Al₂O₃ composites produced by internal oxidation of cast alloys. *Tribol. Mater. Surf. Interfaces* **2009**, *3*, 125–131. [[CrossRef](#)]
36. Hart, R.; Wonsiewicz, B.; Chin, G. High strength copper alloys by thermomechanical treatments. *Metall. Trans.* **1970**, *1*, 3163–3172. [[CrossRef](#)]
37. Chrysanthou, A.; Erbaccio, G. Production of copper-matrix composites by in situ processing. *J. Mater. Sci.* **1995**, *30*, 6339–6344. [[CrossRef](#)]
38. Kolev, M.; Drenchev, L.; Petkov, V. Wear Analysis of an Advanced Al–Al₂O₃ Composite Infiltrated with a Tin-Based Alloy. *Metals* **2021**, *11*, 1692. [[CrossRef](#)]
39. Stanev, L.; Kolev, M.; Drenchev, L. Enhanced Tribological Properties of an Advanced Al–Al₂O₃ Composite Infiltrated with a Tin-Based Alloy. *J. Tribol.* **2021**, *143*, 064502. [[CrossRef](#)]
40. Hoffman, R.; Pan, W.-P. Measuring ΔH using TG—DTA and incorporating mass change into the result. *Thermochim. Acta* **1991**, *192*, 135–146. [[CrossRef](#)]
41. Hoffman, R. Measuring ΔH Using DSC, TGA & DTA. Master's Thesis, Western Kentucky University (WKU), Bowling Green, KY, USA, 1990.
42. Deng, Z.; Yin, H.; Zhang, C.; Zhang, G.; Zhang, T.; Liu, Z.; Wang, H.; Qu, X. Sintering mechanism of Cu-9Al alloy prepared from elemental powders. *Prog. Nat. Sci. Mater. Int.* **2019**, *29*, 425–431. [[CrossRef](#)]
43. Wang, X.; Dong, H.; Liu, J.; Qin, G.; Chen, D.; Zhang, E. In vivo antibacterial property of Ti-Cu sintered alloy implant. *Mater. Sci. Eng. C* **2019**, *100*, 38–47. [[CrossRef](#)] [[PubMed](#)]
44. Ruiz, E.; Achim, V.; Soukane, S.; Trochu, F.; Bréard, J. Optimization of injection flow rate to minimise micro/macro-voids formation in resin transfer molded composites. *Compos. Sci. Technol.* **2006**, *66*, 475–486. [[CrossRef](#)]